HEAT AND MASS TRANSFER FROM MOIST AIR FLOWING INSIDE COLD HORIZONATL CIRCULAR DUCT I-THEORETICAL STUDY

إنتقال الحرارة والكتلة من هواء رطب يمر داخل مجرى دائرى أفقى بارد I- دراسة نظرية

Hesham M. Mostafa[1] and M. G. Mousa[2]

1: Higher Technological Institute, Tenth of Ramadan City, Egypt.

2: Mech. Power Eng. Dept., Faculty of Engineering, Mansoura University, Mansoura, Egypt.

Email :Mgmousa@mans.edu.eg, DrHeshamMostafa@yahoo.com

خلاصة البحث:

فى هذا البحث تم عمل دراسة نظرية لإنتقال الحرارة والكتلة الأنبين لسريان هواء رطب يمر داخل مجرى دائرى أفقى سطحه الخارجى مبرد. لإتمام هذه الدراسة تم إفتراض أن سريان الهواء داخل الأنبوب رقائقى ومستقر وقد تم وضع المعادلات الحاكمة للسريان في صورة تفاضلية لابعدية لحلها عدديا وهذه المعادلات هى معادلة السريان ومعادلة الحركة ومعادلة الطاقة ومعادلة التركيز وذلك باستخدام تعريف مناسب لكل من المتغيرات المستقلة والتابعة. وبحل هذه المعادلات عدديا أمكن الحصول على توزيع كل من السرعة ودرجة الحرارة والتركيز اللابعدي للهواء المار داخل المجرى الدائرى الأفقى. أيضا تم الحصول على رقم نوسلت الموضعى ورقم شيروود الموضعى كدالة فى رقم رينولدز عند مواضع مختلفة على طول المجرى.

وقد أظهرت النتائج أن رقم نوسلت المتوسط ورقم شيروود المتوسط يزيد مع زيادة رقم رينولدز . أيضا رقم نوسلت يزيد مع زيادة رقم براندتل وكذلك رقم شيروود يزيد مع زيادة رقم شميت. وقد تم الحصول على صيغة لكل من رقم نوسلت كدالة فى رقم رينولدز و رقم براندتل وكذلك رقم شيروود كدالة فى رقم رينولدز و رقم شميت. وللتأكد من صلاحية النموذج النظرى تم إجراء مقارنة بين كل من النتائج النظرية الحالية ونتائج معملية من أبحاث أخرى سابقة وكانت نتيجة هذه المقارنة مرضية.

Abstract

Heat and mass transfer from moist air flowing inside cold horizontal circular duct is investigated theoretically. In the present theoretical model, the flow of air inside the cold horizontal circular duct is assumed to be laminar and steady in cylindrical coordinates. The governing equations are the continuity, momentum, energy and concentration equations. These governing equations are put in the dimensionless form. By introducing new proper independent and dependent variables, the governing equations are transformed to a set of dimensionless differential equations. A computer program in FORTRAN language is developed to solve this set of equations to determine the distribution of the dimensionless velocity, temperature and concentration. Also, local values of Nusselt and Sherwood numbers for different values of process parameters are calculated. These parameters are presented by the following dimensionless physical quantities; Prandtl, Schmidt, and Reynolds numbers.

The present results show that, the average values of Nusselt and Sherwood numbers increase with increasing Reynolds number. Nusselt number increases with increasing Prandtl number. Also, Sherwood number increases with increasing Schmidt number. Comparison between the obtained theoretical results and the previous experimental works show good agreement.

Keywords: Heat and mass transfer, Steady, Laminar Flow, Moist air and Horizontal circular duct.

NOMENCLATURE

C	Concentration of water vapor in the flowing air	kg/m^3
C^*	Dimensionless concentration, $C^* = \frac{C - C_\infty}{C_w - C_\infty}$	--

Accepted November 20, 2006

C_p	Specific heat at constant pressure	J/kg K
D	Diffusion coefficient	m^2/s
h	Heat transfer coefficient	$W/(m^2.K)$
h_m	Mass transfer coefficient	m/s
h_{fg}	Latent heat of condensation	J/kg
k	Thermal conductivity	W/m.K
l	Length of cold horizontal duct	m
L	Dimensionless length, L/ro	--
Nu	Nusselt number , $Nu = \frac{h\ ro}{k}$	--
p	Pressure	Pa
Pe	Peclet number, Pe=Re Pr	--
Pr	Prandtl number, $Pr = \frac{cp\mu}{k}$	--
q	Heat flux	W/m^2
Re	Reynolds number, $Re = \frac{u_f\ ro}{\upsilon}$	--
r_o	Radius of the duct	m
Sc	Schmidt number, $Sc = \frac{\upsilon}{D}$	--
Sh	Sherwood number, $Sh = \frac{h_m \cdot ro}{D}$	--
T	Temperature	K
T_w	Wall temperature	K
T_∞	Ambient temperature	K
u, w	Velocity components in r- and z- directions	m/s
U, W	Dimensionless velocity components in R- and Z-directions	--
r, z	Radial and axial coordinates	m
R, Z	Dimensionless radial and axial coordinates, R=r/ro, Z=z/ro	--

Greek Symbol

α	Thermal diffusivity	m^2/s
ψ	Stream function	m^3/s
μ	Dynamic viscosity of fluid	kg/m.s
ν	Kinematics viscosity of fluid	m^2/s
ρ	Density	kg/m^3
θ	Dimensionless temperature; $\theta = \frac{T - T_w}{T_\infty - T_w}$	--

Subscript

av :	*average*	w :	wall	v	vapor
i :	*inlet*	∞ :	free stream	*l*	*humid air*
2	*condensate*				

1. INTRODUCTION

Humid-air flows in ducts are often used in various technical applications. Humidity control systems, air cleaning and conditioning systems, and also apparatus for drying materials in humid gases are some examples of these applications. If the

temperature of the streamline surface is lower than the saturation point, then the steam contained in the air undergoes condensation. In this case, the total wall heat flux includes the component due to convection, spent on cooling the vapor–gas mixture in the boundary layer, and the phase-transition heat, spent on vapor condensation. Heat and mass transfer processes through air-water interfaces are of a major importance in many engineering applications.

Lee et al. (2006) studied a series of experiments was performed to investigate the local heat transfer phenomenon inside a U-tube in a reflux condensation mode. A total of 477 data (108 for pure steam flow conditions and 369 for steam–air flow conditions) for the local heat transfer coefficients were obtained for various inlet flow rates of steam and air under atmospheric conditions. Based on the steam–air experimental results, a new correlation applicable to the reflux condensation mode is developed using the degradation factor.

Jenny Lindblom and Bo Nordell, (2006) studied the condensation irrigation (CI) which is a combined system for desalination and irrigation. By evaporating seawater in, for example, solar stills and letting the humidified air transport the formed vapour into an underground pipe system, fresh water will precipitate as the air is cooled by the ground. By using drainage pipes for underground air transportation, perforations in the pipes enable the water to percolate into the soil.

Revankar and Ollock, (2005) studied a two-dimensional, steady state model of convective film-wise condensation of a vapor and condensable gas mixture flowing downward inside a vertical tube. The mass transfer at the film and gas interface is treated as diffusion controlled process. The non-condensable effect on the condensation is taken into account through boundary layer analysis of species concentration and energy balance. Numerical predictions were obtained for the condensation heat transfer coefficient of turbulent vapor flow associated with laminar condensate. The predicted results were compared with the experimental data in the literature to assess the model. Non-condensable mass fraction and vapor non-condensable mixture temperature were presented in the form of radial and axial profiles.

Volchkov et al. (2004) studied the numerical solution of the system of differential energy, diffusion, and boundary-layer flow equations for the laminar and turbulent flows of humid air with surface. Steam condensation shows that the momentum- and matter-transfer processes and the convective heat transfer are similar with allowance for the standard corrections for the Prandtl and Lewis numbers in the range of steam concentrations in the flow core $0<C_0\leq 0.2$. Heat and mass transfer in humid air with such steam concentrations obeys the "dry-wall" regularities. The total heat transfer on the wall can be substantially increases due to the phase-transition heat; with increasing moisture content, the heat-transfer intensification ratio also increases.

Thome et al. (2003), studied a new flow pattern map and flow pattern based heat transfer model for condensation inside horizontal plain tubes. In Part I, a new version of a two-phase flow pattern map, originally for flow boiling, is presented for condensation inside horizontal tubes while a new heat transfer model is presented in Part II. The new flow pattern map incorporates a newly defined logarithmic mean void fraction (LMe) method for calculation of vapor void fractions spanning from low pressures up to pressures near the critical point. Several other modifications are also made that are appropriate for condensation as opposed to evaporation. In the absence of void fraction data at high reduced pressures for these conditions, the new LMe method has been indirectly validated using the convective condensation model for annular flow and

corresponding heat transfer test data at reduced pressures up to 0.8 bar. The new map has also been successfully compared to some recent

Sarma et al. (2002) solved analytically the problem of convective condensation of vapors inside a horizontal condenser tube. Homogeneous model approach is employed in the estimation of shear velocity, which is subsequently, made use of in predicting local convective condensation heat transfer coefficients. There results are compared with some of the available equations in the literature. It is observed that the agreement is reasonably satisfactory validating the assumptions and the theory presented.

In most engineering applications, heat and mass transfer occur simultaneously and often these are strongly coupled. Therefore, in the present work, numerical study of heat and mass transfer from moving moist air flowing inside a horizontal cooled circular duct with constant wall temperature is examined.

2. MATHEMATICAL MODEL

A schematic of physical model under study is shown in Fig.(1), which shows the coordinate system and dimensional nomenclature. The fluid flow is assumed to be axi-symmetric flow, laminar, and steady with constant properties for the range of temperatures considered, two dimension, and compressible. Before contact, the velocity and temperature of fluids are uniform and correspond to free stream conditions.

The effect of gravity force and heat dissipation is neglected. Moreover, uniform velocity and temperature profiles, at the inlet of the circular duct, are assumed.

2.1 Governing Equations

It is suitable to select the cylindrical coordinate (r, ϕ, z) to express the flow governing equations. The used coordinate system is shown in figure (1). The flow describing equations are continuity, momentum, energy and concentration equations for axi-symmetric. They can be written as:

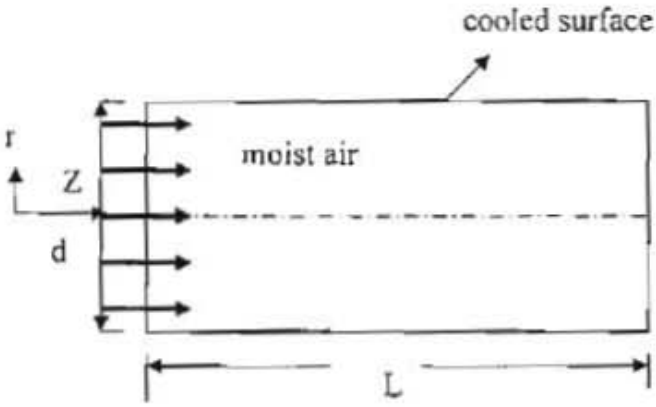

Fig.(1) schematic diagram of the problem

$$\frac{1}{r}\frac{\partial(ru)}{\partial r}+\frac{\partial w}{\partial z}=0 \quad \ldots\ldots(1)$$

$$w\frac{\partial w}{\partial z}+u\frac{\partial w}{\partial r}=-\frac{1}{\rho}\frac{\partial p}{\partial z}+\frac{\mu}{\rho}\left(\frac{\partial^2 w}{\partial r^2}+\frac{1}{r}\frac{\partial w}{\partial r}+\frac{\partial^2 w}{\partial z^2}\right) \quad \ldots\ldots(2)$$

$$w\frac{\partial u}{\partial z}+u\frac{\partial u}{\partial r}=-\frac{1}{\rho}\frac{\partial p}{\partial r}+\frac{\mu}{\rho}\left(\frac{\partial^2 u}{\partial r^2}+\frac{1}{r}\frac{\partial u}{\partial r}-\frac{u}{r^2}+\frac{\partial^2 u}{\partial z^2}\right) \quad \ldots\ldots(3)$$

$$w\frac{\partial T}{\partial z}+u\frac{\partial T}{\partial r}=\frac{k}{\rho C_p}\left(\frac{\partial^2 T}{\partial r^2}+\frac{1}{r}\frac{\partial T}{\partial r}+\frac{\partial^2 T}{\partial z^2}\right) \quad \ldots\ldots(4)$$

$$w\frac{\partial C}{\partial z}+u\frac{\partial C}{\partial r}=D\left(\frac{\partial^2 C}{\partial r^2}+\frac{1}{r}\frac{\partial C}{\partial r}+\frac{\partial^2 C}{\partial z^2}\right) \quad \ldots\ldots(5)$$

Equations (1-5) are the continuity equation, axial and radial momentum equations, energy equation and concentration equation respectively. Where; w and u are the velocity component in axial and radial directions. The temperature, density and specific heat of the fluid at constant pressure are denoted by T, ρ and C_p; respectively. In the forgoing equations, P, μ, k, D and C are pressure, dynamic viscosity, thermal conductivity of the fluid, mass diffusivity; and concentration respectively.

The flow, heat and mass transfer inside the circular duct for laminar and steady flow are considered. In this case, the corresponding continuity, momentum, energy and concentration equations (1 – 5) in cylindrical coordinates must satisfy the following boundary conditions, as ;

At $z = 0.0$, $0.0 \le r \le r_o$:

$w = w_o$, $u = 0.0$, $T = T_\infty$, $C = C_\infty$

at $0.0 < z < l$, $r = r_o$

$w = u = 0.0$, $T = T_w$, $C = C_w$

at $z = l$, $0.0 \le r \le r_o$

$$\frac{\partial w}{\partial z} = 0.0,\ u = 0.0,\ \frac{\partial T}{\partial r} = 0.0,\ \frac{\partial C}{\partial r} = 0.0 \quad (6)$$

for interface

$$k_1 \frac{\partial T_1}{\partial r} = k_2 \frac{\partial T_2}{\partial r} + \rho_1 D h_{fk} \frac{\partial m_v}{\partial r}$$

- At Axis of Symmetry at r=0, 0<z<l

$$\frac{\partial w}{\partial r} = \frac{\partial u}{\partial r} = \frac{\partial T}{\partial r} = \frac{\partial C}{\partial r} = 0.0$$

Where; T_∞ and C_∞ are the temperature and water vapor concentration in ambient air.

Solving the governing equations (1-5) with their boundary conditions equation (6), one can obtain the velocity, temperature and concentration distributions through the flow field. Knowing hydrodynamic and thermal flow field local heat and mass transfer coefficients, and in turn, local Nusselt and Sherwood numbers can be determined. Local heat and mass transfer coefficients are defined according to the following equations;

$$h = \frac{q}{T_w - T_\infty} = \frac{-k\left(\frac{\partial T}{\partial r}\right)_{@r=r_o}}{T_w - T_\infty} \ ;$$

$$h_m = \frac{m'}{C_w - C_\infty} = \frac{-D\left(\frac{\partial C}{\partial r}\right)_{@r=r_o}}{C_w - C_\infty} \ . \quad (7\text{-a})$$

And consequently local Nusselt and Sherwood numbers can be expressed as;

$$Nu = \frac{h.r_o}{k},\ Sh = \frac{h_m.r_o}{D} \quad \ldots . (7\text{-b})$$

Average Nusselt and Sherwood numbers can be expressed as;

$$Nu_{av} = \left(\frac{1}{l}\right).\int_0^l Nu.dz \ ,$$

$$Sh_{av} = \left(\frac{1}{l}\right).\int_0^l Sh.dz \quad \ldots . (7\text{-c})$$

Equation (7-a) expresses local heat transfer coefficient h as a function of heat flux at plate q, the duct wall temperature T_w and the temperature of flow T_∞ and local mass transfer coefficient h_m as a function of mass flux of moist air m', the concentration at surface C_w and concentration of moist air flow C_∞. Referring to the definition of local Nusselt and Sherwood numbers, r_o is the air flow passage radius. Referring to the definition of the average Nusselt and Sherwood numbers equation (7-c), l is the distance along z-axis corresponding to duct length.

For eliminating pressure term from above momentum equations (2-3), one introduces flow vorticity ω and stream function ψ, where ω and ψ take the following definitions:

$$u=\frac{1}{r}\frac{\partial\psi}{\partial z}\quad ,\ w=-\frac{1}{r}\frac{\partial\psi}{\partial r},\ \omega=\left(\frac{\partial w}{\partial r}-\frac{\partial u}{\partial z}\right)$$

Substitution with ω, ψ in equations (1-5) and with some manipulations, they can be rewritten as:

$$\frac{1}{r}\frac{\partial\psi}{\partial z}\left(\frac{\partial\omega}{\partial r}-\frac{\omega}{r}\right)-\frac{1}{r}\frac{\partial\psi}{\partial r}\frac{\partial\omega}{\partial z}= \frac{\mu}{\rho}\left\{\frac{\partial^2\omega}{\partial z^2}+\frac{\partial^2\omega}{\partial r^2}+\frac{1}{r}\frac{\partial\omega}{\partial r}-\frac{\omega}{r^2}\right\} \quad \ldots\ldots (8)$$

$$\omega=-\left(\frac{1}{r}\frac{\partial^2\psi}{\partial r^2}-\frac{1}{r^2}\frac{\partial\psi}{\partial r}+\frac{1}{r}\frac{\partial^2\psi}{\partial z^2}\right)\quad \ldots \quad (9)$$

$$-\frac{1}{r}\frac{\partial\psi}{\partial r}\frac{\partial T}{\partial z}+\frac{1}{r}\frac{\partial\psi}{\partial z}\frac{\partial T}{\partial r}= \alpha\left\{\frac{\partial^2 T}{\partial z^2}+\frac{1}{r}\frac{\partial T}{\partial r}+\frac{\partial^2 T}{\partial r^2}\right\}\quad \ldots\ldots (10)$$

$$-\frac{1}{r}\frac{\partial\psi}{\partial r}\frac{\partial C}{\partial z}+\frac{1}{r}\frac{\partial\psi}{\partial z}\frac{\partial C}{\partial r}= D\left\{\frac{\partial^2 C}{\partial z^2}+\frac{1}{r}\frac{\partial C}{\partial r}+\frac{\partial^2 C}{\partial r^2}\right\}\quad \ldots\ldots (11)$$

Equations (8-11) must satisfy the following boundary conditions;

- *For* $z=0.0,\ 0.0\le r\le r_o$:

$$\frac{1}{r}\frac{\partial\psi}{\partial r}=-w_0,\ \frac{\partial\psi}{\partial z}=0.0,\ T=T_o,\ C=C_o$$

- *For* $0.0<z<l,\ r=r_o$:

$$\frac{\partial\psi}{\partial r}=0,\ T=T_w,\ C=C_w$$

at Axis of Symmetry $r=0$, $0<z<l$ ..... (12)

$$\frac{\partial}{\partial z}\left(\frac{1}{r}\frac{\partial\psi}{\partial r}\right)=\frac{\partial}{\partial r}\left(\frac{1}{r}\frac{\partial\psi}{\partial z}\right)=0,\ \frac{\partial T}{\partial r}=\frac{\partial C}{\partial r}=0.0$$

- *For* $0.0<z<l$, (interface) :

$$k_1\frac{\partial T_1}{\partial r}=k_2\frac{\partial T_2}{\partial r}+\rho_1 D h_{fg}\frac{\partial m_v}{\partial r}$$

Where 1 refer to moist air flow and 2 refer to condensate water.

2.2 Dimensionless Form of the Governing Equations

To put the flow describing equations in dimensionless form, one introduces the following definitions of the dependent and independent variables as:

$$\theta=\frac{T-T_w}{T_o-T_w},\ \Psi=\frac{\psi}{w_o r_o^2},\ \Omega=\frac{\omega}{w_o/r_o},$$

$$W=\frac{w}{w_o},\ U=\frac{u}{w_o},\ R=\frac{r}{r_o},\ Z=\frac{z}{r_o},\quad (13)$$

$$L=\frac{l}{r_o},C^*=\frac{C-C_w}{C_o-C_w}$$

Where the dimensionless temperature, the dimensionless stream function the dimensionless vorticity and dimensionless concentration are denoted by θ, Ψ, Ω *and* C^* respectively. W and U are the dimensionless axial and radial velocities respectively. The dimensionless duct length is denoted by L. The dimensionless cylindrical coordinates and the dimensionless distance are denoted as R and Z respectively.

Reynolds, Prandtl Schmidt and Peclet numbers in the following sections are denoted as Re, *Pr*, Sc and *Pe* respectively, they are defined according to the following relations:

$$Re=\frac{\rho w_o r_o}{\mu},\quad Pr=\frac{\nu}{\alpha}\quad Sc=\frac{\nu}{D}\quad \text{and}$$

$Pe=Re.Pr$ or $Pe_c=Re\ Sc$ ....(14)

Using the above dimensionless forms of the dependent and independent variables (13) and the dimensionless previously mentioned numbers (14), the dimensionless form of the momentum, vorticity, energy, and concentration equations can be rewritten as:

$$\left\{\frac{\partial\Psi}{\partial R}\frac{\partial\Omega}{\partial Z}-\frac{\partial\Psi}{\partial Z}\left(\frac{\partial\Omega}{\partial R}-\frac{\Omega}{R}\right)\right\}= \frac{R}{\mathrm{Re}}\left(\frac{\partial^2\Omega}{\partial Z^2}+\frac{\partial^2\Omega}{\partial R^2}+\frac{1}{R}\frac{\partial\Omega}{\partial R}-\frac{\Omega}{R^2}\right) \quad \ldots\ldots(15)$$

$$\Omega=\frac{-1}{R}\left(\frac{\partial^2\Psi}{\partial R^2}-\frac{\partial\Psi}{R\partial R}+\frac{\partial^2\Psi}{\partial Z^2}\right) \quad \ldots\ldots(16)$$

$$\left(\frac{\partial\Psi}{\partial R}\frac{\partial\theta}{\partial Z}-\frac{\partial\Psi}{\partial Z}\frac{\partial\theta}{\partial R}\right)= \frac{R}{\mathrm{Pe}}\left(\frac{\partial^2\theta}{\partial R^2}+\frac{1}{R}\frac{\partial\theta}{\partial R}+\frac{\partial^2\theta}{\partial Z^2}\right) \quad \ldots\ldots(17)$$

$$\left(\frac{\partial\Psi}{\partial R}\frac{\partial C^*}{\partial Z}-\frac{\partial\Psi}{\partial Z}\frac{\partial C^*}{\partial R}\right)= \frac{R}{\mathrm{Pe}_s}\left(\frac{\partial^2 C^*}{\partial R^2}+\frac{1}{R}\frac{\partial C^*}{\partial R}+\frac{\partial^2 C^*}{\partial Z^2}\right) \quad \ldots(18)$$

The dimensionless equations (15-18) must satisfy the following boundary conditions;

- For $Z=0.0,\ 0.0\le R\le 1$:

$$\frac{\partial\Psi}{\partial R}=-R,\ \frac{\partial\Psi}{\partial Z}=0,\ \theta=0,\ C^*=0$$

- For $0.0<Z<L,\ R=1$:

$$\frac{\partial\Psi}{\partial R}=0.0,\ \theta=1,\ C^*=1$$

- For $0.0<Z<L,\ R=1$:

$$\frac{\partial}{\partial R}\left(\frac{1}{R}\frac{\partial\Psi}{\partial R}\right)=0,\quad \left(\frac{\partial\Psi}{\partial Z}\right)=0,\quad \frac{\partial\theta}{\partial R}=0,\quad C^*=0.0 \quad \ldots\ldots(19)$$

- for $R=0.0,\ Z=L$

$$\frac{\partial}{\partial Z}\left(\frac{1}{R}\frac{\partial\Psi}{\partial R}\right)=\frac{\partial}{\partial R}\left(\frac{1}{R}\frac{\partial\Psi}{\partial Z}\right)=0,\ \frac{\partial\theta}{\partial R}=\frac{\partial C^*}{\partial R}=0$$

- For interface :

$$k_1\frac{\partial\theta_1}{\partial R}=k_2\frac{\partial\theta_2}{\partial R}+\frac{\rho_1 D h_{fg}}{\Delta T}\frac{\partial C^*}{\partial R}$$

One can solve equations (11-13) with the aid of boundary condition equations to obtain the dimensionless velocity and temperature distribution through out the flow field. Consequently and with the aid of equation (8), the local Nusselt number can be derived as a function of dimensionless temperature as:

$$Nu=\left(\frac{1}{\theta-1}\right)\left(\frac{d\theta}{dR}\right)_{@R=1}$$

$$Sh=\left(\frac{dC^*}{dR}\right)_{@R=1} \quad \ldots\ldots(20)$$

2.3 NUMERICAL TECHNIQUE

Considering a mesh covering the domain of the flow field with lines parallel to the R - axis and Z-axis; and with uniform step size, each node of the mesh is identified by two identifiers i and j, as shown in Fig. (2). Considering the R -direction, the value of R at any row $i+1$, can be evaluated according to the following relations:

$$R_{i+1}=R_i+\Delta R$$

Where i varies from 1 corresponding to $R=0$, to M corresponding to $R=1$, where the total number of rows equal to M. ΔR is the value of step size in R – direction. It is clear that, ΔR depends on the selected total number of rows M and the maximum distance in R direction. In the same manner, the value of Z at any column $j+1$ can be evaluated according to the following relation:

$$Z_{j+1}=Z_j+\Delta Z$$

Where j varies from 1 corresponding to $Z=0$, to N corresponding to $Z=L$ and the step size in Z – direction which depends on the number of columns N and the maximum distance in Z direction.

The partial differential forms of the governing equations are transformed to sets of linear algebraic equations. Solving these sets of equations, using Gauss-Siedel iterative method, the hydrodynamic, the thermal and concentration flow fields can be obtained. Consequently, local and average Nusselt and Sherwood numbers can be derived with the aid of their definitions.

2.4 Numerical Procedure

The systems of algebraic equations are solved using Gauss-Siedel iteration method with the above technique. The calculations are carried out on uniform grid size

distribution. A uniform grid with (6000*200) is considered to give grid independent results.

Because finite difference technique is used to solve the momentum and energy equations, the solution can become unstable, i.e., as the solution proceeds; it might diverge increasingly from the actual solution. A simplified analysis of the conditions under which instability occurs is established, the results obtained indicate that convergence exists if:

$$\Delta R \ \alpha \ \overline{\Delta Z}^{2}.\mathrm{Re}$$

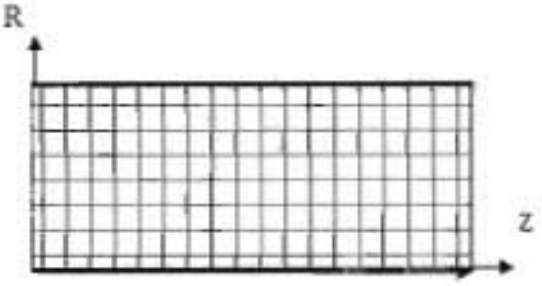

Fig.(2) schematic diagram of the mesh used in calculation

The solution is carried out row by row. Seeking for rapid convergence of the solution, the obtained value of (Ω, Ψ, θ, and C^*) is used in the rest of equations of the rest (Ω, Ψ, θ, and C^*)'s. This iteration is continued till either the percentage relative error is equal to or less than the prescribed allowable error (maximum error $\leq 1*10^{-7}$).

Accordingly, the hydrodynamic and temperature distributions of the flow are obtained. The velocities and local Nusselt and Sherwood numbers can obtained at any general point i,j as;

Axial velocity, $W = -\frac{1}{R_i}\frac{\Psi_{i+1,j}-\Psi_{i-1,j}}{2\Delta R}$, radial velocity, $U = \frac{1}{R_i}\frac{\Psi_{i,j+1}-\Psi_{i,j-1}}{2\Delta Z}$,

Nusselt number, $Nu = \left(\frac{1}{\theta - 1}\right)\left(\frac{\theta_{i,n}-\theta_{i,n-1}}{\Delta R}\right)$,

Sherwood number, $Sh = -\left(\frac{C^*_{i,n}-C^*_{i,n-1}}{\Delta R}\right)$

3. Results and Discussion

Figure (3) Illustrates the flow pattern for the flow issues inside a circular duct at Re = 2500 and 5000. The streamlines show that at Re=2500 the flow issues inside the duct is going parallel to the duct wall rapidly. At Re= 5000 the duct length is larger for low Reynolds number values of stream lines inside the duct were found.

Figure (4) illustrates the isothermal contours for the flow issues inside a circular duct at Re = 2500 and 5000. The temperature distribution denotes that the flow temperature is lower at the upper wall and get higher far from the upper wall as expected.

Figure (5) illustrates the isomass contours for the flow issues inside a circular duct at Re = 2500 and 5000. The concentration distribution denotes that the flow concentration is high at the wall and get poor far from the lower wall as expected.

The accuracy of numerical model is verified by comparing the results from present model with the corresponding results reported by Lee et al. (2006) and Sarma et al. (2002). Figure (6) shows the variation of the average Nusselt number with Reynolds number for the present work compared with results obtained by Lee et al. (2006). It is noticed that for the present work Nusselt number increases with increasing Reynolds number.It is observed that good agreement was obtained.

Figure (7) shows the variation of the average Sherwood number with Reynolds number for the present work compared with results obtained by Sarma et al. (2002). It is observed that for the present work Sherwood number increases with increasing Reynolds number. The present results show good agreement with the results of previous work.

Figure (8) shows the variation of local Nusselt with respect to dimensionless distance Z at different values of Prandtl number. It is observed that, as Prandtl number increases the value of Nusselt number also increases.

Local Sherwood number is plotted against dimensionless distance Z with different values of Schmidt number, as shown in Fig. (9). It is observed that, as Schmidt number increases the value of Sherwood number increases.

The following relations correlate the theoretical results, where the Nusselt and Sherwood numbers are expressed as functions of Reynolds, Prandtl and Schmidt numbers:

$$Nu = 1.145\, Re^{0.64}\, Pr^{0.34}$$

$$Sh = 1.252\, Re^{0.612}\, Sc^{0.34}$$

Conclusions

In the present study, the condensation process of water vapor from moist air is, theoretically analyzed. The effects of process parameters are investigated. These parameters are presented by the following dimensionless physical quantities; Prandtl, Schmidt, and Reynolds numbers. Considering the theoretical proposed model, it is found that the increase of Prandtl and Schmidt numbers cause increase of Nusselt and Sherwood numbers.

Comparison between the obtained results and the previous works in case of steady flow shows good agreement. Two correlations for Nusselt number and Sherwood numbers are obtained.

REFERENCES

[1] **Lee, K. W., NO, H. C., Chu, I. C., Moon, Y. M., and Chun, M. H.**, (2006) "Local heat transfer during reflux condensation mode in a U-tube with and without non-condensable gases", International Journal of Heat and Mass Transfer Vol. 49, pp. 1813–1819.

[2] **Revankar, S. T., and Ollock, D.**, (2005), "Laminar film condensation in a vertical tube in the presence of non-condensable gas", Applied Mathematical Modeling, Vol. 29, pp. 341–359.

[3] **Hammou, Z. A., Benhamou, B., Galanis, N. and Orfi, J.**, (2004), "Laminar mixed convection of humid air in a vertical channel with evaporation or condensation at the wall", Int. J. Thermal Sciences, Vol. 43, pp. 531-539.

[4] **Volchkov, E. P., Terekhov, V. V., and Terekhov V. I.** (2004), "A numerical study of boundary-layer heat and mass transfer in a forced flow of humid air with surface steam condensation", International Journal of Heat and Mass Transfer, Vol. 47, Issues 6-7, pp. 1473-1481.

[5] **Thome, J. R., El Hajal, J., Cavallini, A.**, (2003), "New heat transfer model based on flow regimes condensation in horizontal tubes, part 2" International Journal of Heat and Mass Transfer Vol. 46, pp.3365–3387.

[6] **Sarma, P. K., Sastry, C. V. N., Rao, V. D., Kakac, S., and Liu, H.**, (2002), "Convective condensation heat transfer in a horizontal condenser tube" Int. J. Thermal Sciences Vol. 41, pp. 295–301.

[7] **Lee, K. T., (1998)** " Mixed convection heat transfer in horizontal rectangular ducts with wall transpiration effects" Int. J. Heat Mass Transfer, Vol. 41, No. 2, pp. 411- 423

[8] **Borgnakke, C. and Sonntay, R. E.**, (1997), "Table of Thermodynamic and transport Properties," John Wiley & sons Inc.

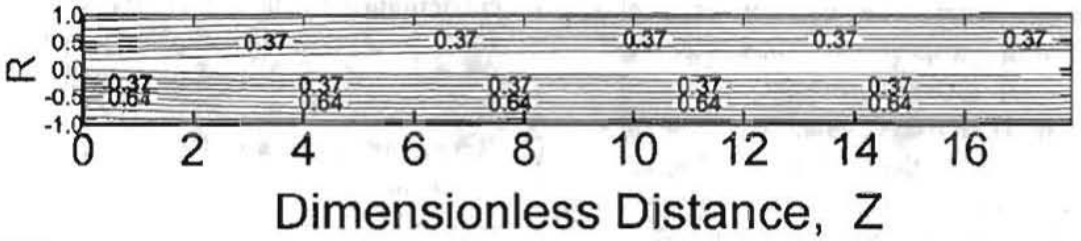

Re=2500

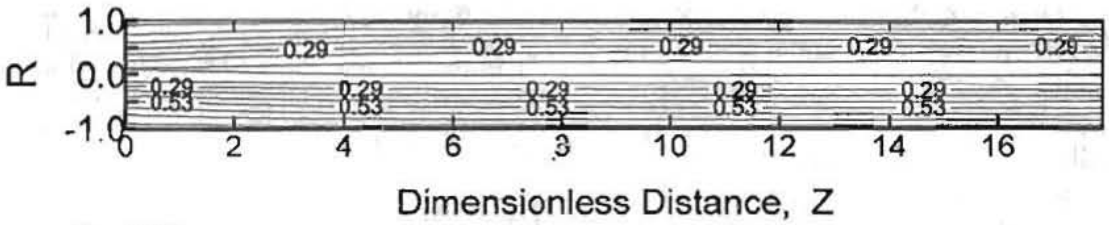

Re=5000

Figure (3) Stream lines for different Reynolds number

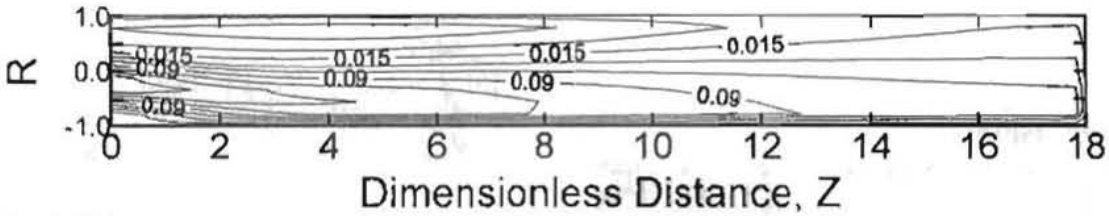

Re=2500

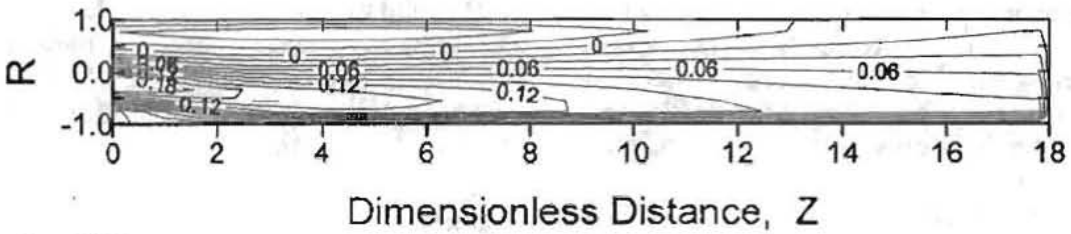

Re=5000

Figure (4) Isotherm lines for different Reynolds number

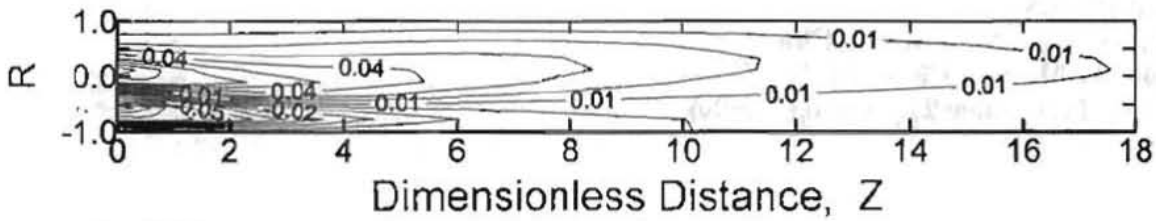

Re=2500

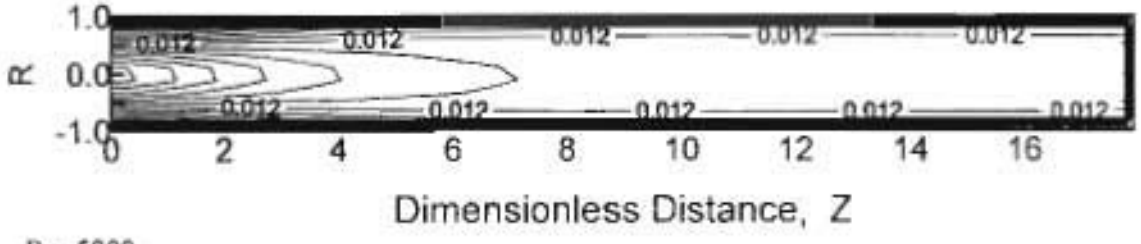

Re=5000

Figure (5) Iso-mass lines for different Reynolds number

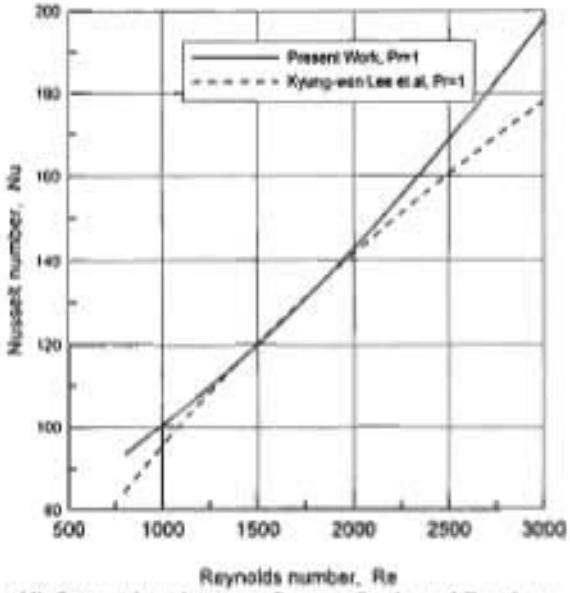

Fig.(6) Comparison between Present Study and Previous work

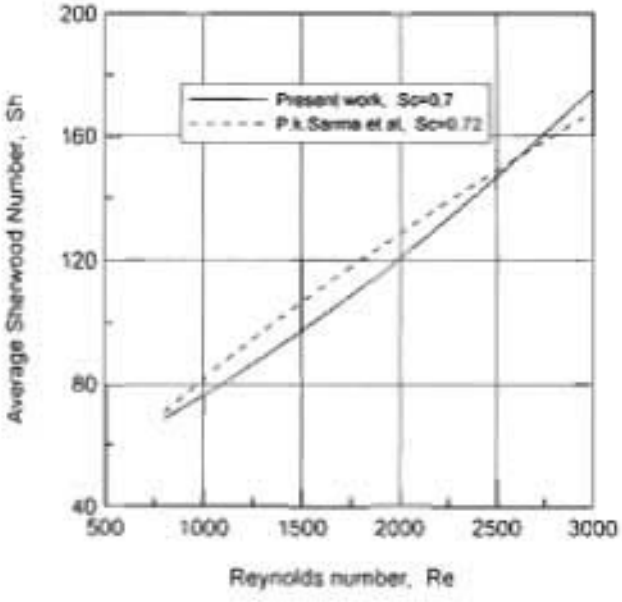

Fig.(7) Comparison between Average Sherwood number

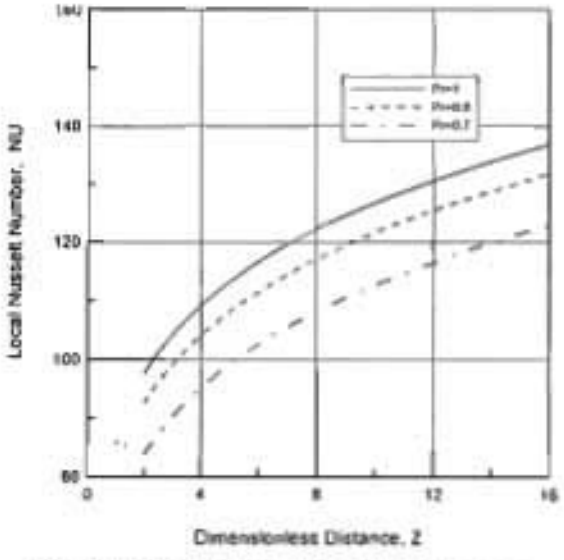

Fig.(8) Effect of Prandtl number on local Nusselt number at Re=2500

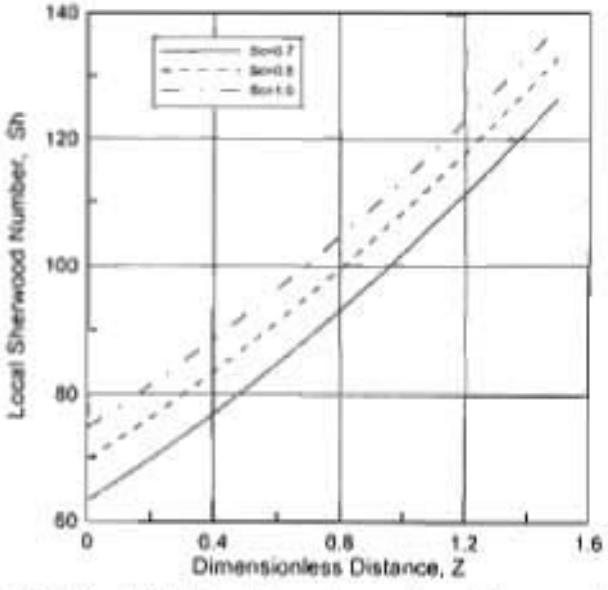

Fig.(9) Effect of Schmidt number on local Sherwood number at Re=2500